ECONOMICAL AND ACCURATE METHODS FOR MEASURING THE MULTIPOLE FIELD COEFFICIENTS OF BENDING MAGNETS AND QUADRUPOLES

K.-D. Lohmann
CERN, Geneva, Switzerland

Abstract

All relevant field parameters of bending magnets and quadrupoles can be measured with long straight coils, if the curvature of the particle trajectories inside these elements is not too great.

The particular problems related to long coils are discussed, namely calibration, measuring errors, and mechanical layout. The measuring apparatus used for the CERN Proton Synchrotron booster magnets is discussed, comprising:

1. The long coil system for measuring bending magnets of 1.6 m length and 0.07 m gap height, featuring:

- simultaneous measurement in three planes;
- coil flipping with pneumatic motors;
- 0.003% relative accuracy;
- simple mechanical construction.

2. The harmonic coil with compensation winding for measuring the quadrupoles.

All multipole coefficients up to 28-pole ones are measured with an accuracy of 0.003% (multipole field referred to the quadrupole field at bore radius). The displacement of the magnetic centre with respect to the geometric centre of the quadrupole is measured to within 0.01 mm.

The system requires neither a precise angular position nor precise incremental rotation.

1. Introduction

What magnitude of non-linearities in the magnetic field of bending magnets and quadrupoles can be accepted for a particular project (beam transport or accelerator magnet system)?

To answer this question, one has to find a mathematical model for the magnets which includes these non-linearities, and then compute the particle trajectories. The mathematical model used for the design of the PS Booster[1] was the so-called three-thin-lens approach[2], where one lens corresponds to the field inside the magnet and two lenses simulate the end fields.

If one has a complete field map of the magnet, one can compare the calculated particle trajectories in the real magnet to those in the three-lens model. The differences found could safely be neglected in the case of the PS Booster[3], where the bending angle of the magnet is 11.25°.

For the existing beam simulation[2], the field non-linearities have to be entered into the program in terms of multipole coefficients of a bi-dimensional field. The three-lens model leads to a measuring method using long straight coils subdivided longitudinally into three parts. The measuring points were chosen such that the multipole coefficients could be extracted with the highest accuracy, i.e. at the outer boundary of the volume to be measured[4]. For the quadrupole, this field volume is a cylinder; we therefore used a harmonic coil giving the multipole coefficients directly. For the bending magnet, the field volume of interest is a rectangular box of 0.07 × 0.15 × 1.6 m which had to be explored following Cartesian coordinates. The multipole coefficients in this case are extracted from the measurements by fitting the measuring points with polynomials satisfying the Laplace equation.

Using these methods, the number of measuring points could be limited to a reasonable amount, and simple mechanical devices with only one degree of freedom could be used.

2. Measurement of the bending magnets

2.1 Mechanical construction of the measuring apparatus

Figure 1 shows the measuring coil assembly consisting of nine single coils located on three parallel axes. Using the three coils of 1.3 m length inside the iron yoke, we can measure longitudinal average values of the bi-dimensional field. By series connection, we can employ three 2.7 m long coils measuring the bending power $\int B_z \, ds$ on straight parallel lines.

The coils are flipped simultaneously by means of pneumatic motors with hydraulic damping. The rotary movement is transmitted to the three coils by an accurate gear drive. The rotation angle of 180° can be adjusted on the motor itself.

The 2.7 m long coil is carried in five nylon bearings and care has to be taken to avoid vibrations during the flipping movement. The bearings must be short and the whole 2.7 m long coil must be fairly straight. Referring to Fig. 2 one can see that the whole assembly forms a rather stiff rod of 16 kg weight. It simply rests on the pole face of the magnet and needs only to be positioned in the x-direction.

This is done by a rack and pinion drive fixed against the magnet (see Fig. 2). The x-position is encoded by microswitches.

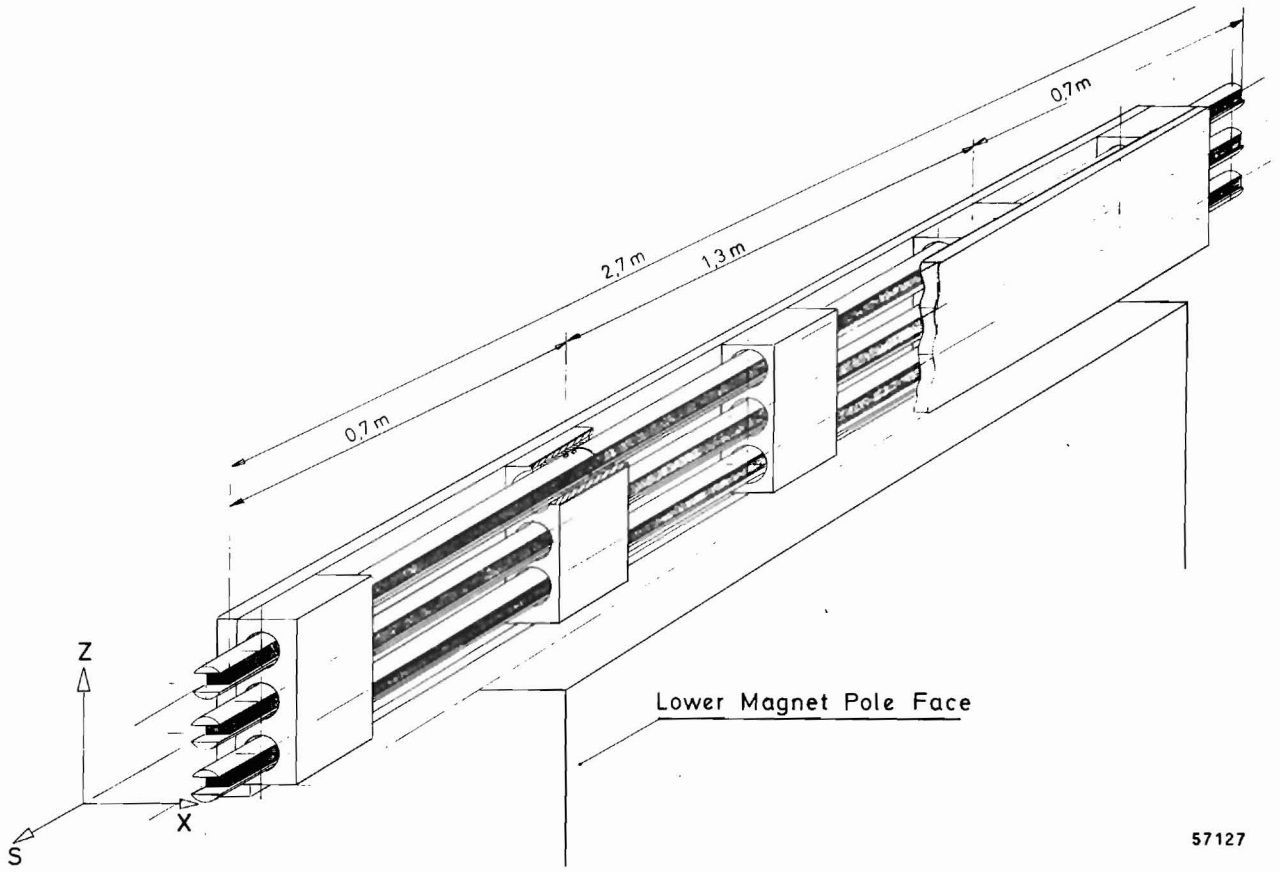

Fig. 1 Long coil assembly consisting of nine individual coils. The pneumatic motor is not shown.

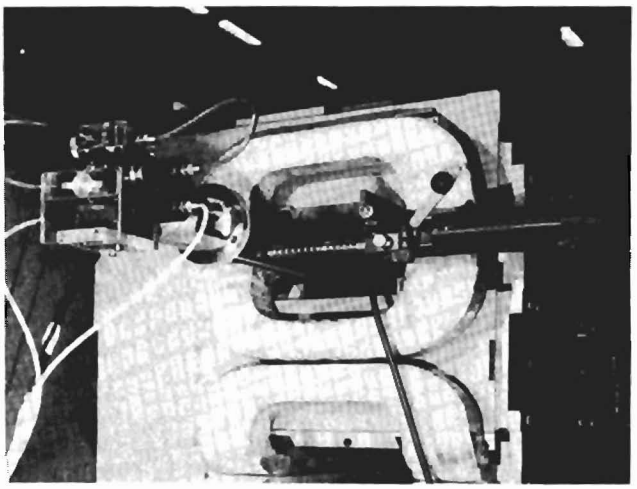

Fig. 2 Long coil assembly with positioning device

2.2 Calibration

The calibration of a package of long coils is not as simple as short coil calibrations. What we would like to have is that the time integral of the coil voltage u_c be proportional to the bending power of the magnet:

$$\int_{t_0}^{t_1} u_c \, dt = \left[K \cdot \int_{s_1}^{s_2} B_z(s,t) \, ds \right]_{t_0}^{t_1} \qquad (1)$$

The actual relationship is more complicated. A good approximation for the coil flux is obtained considering a single loop with variable conductor distance w(s):

$$\int_{t_0}^{t_1} u_c \, dt = \left[-n \int_{s_1}^{s_2} w(s) \cdot B_z(s,t) \, ds \right]_{t_0}^{t_1} \qquad (2)$$

For accurate calibrations, the conductor distance w cannot be considered as a constant, especially if the long coil consists of several parts with gaps in between. So, a universal coil constant K, independent of B(s), does not exist. The equivalent average w for a particular field shape B(s) may be obtained by one of the following methods:

a) Measurement of the coil surface area $A = n \cdot \bar{w} \cdot \ell_c$ of every individual coil. The coil winding length ℓ_c, as well as the intercoil gaps, may be determined by mechanical measurements. Assuming a simple function B(s), e.g. a linear fringe field approximation, one can determine $\bar{w}$ as a function of the equivalent length of the magnet.

b) Calibration in a long magnet by longitudinal displacement of the coil according to Fig. 3. By this method, average values of w(s) may be determined for any longitudinal interval of the coil. The method requires a long magnet with uniform field inside and a fringe field as short as possible.

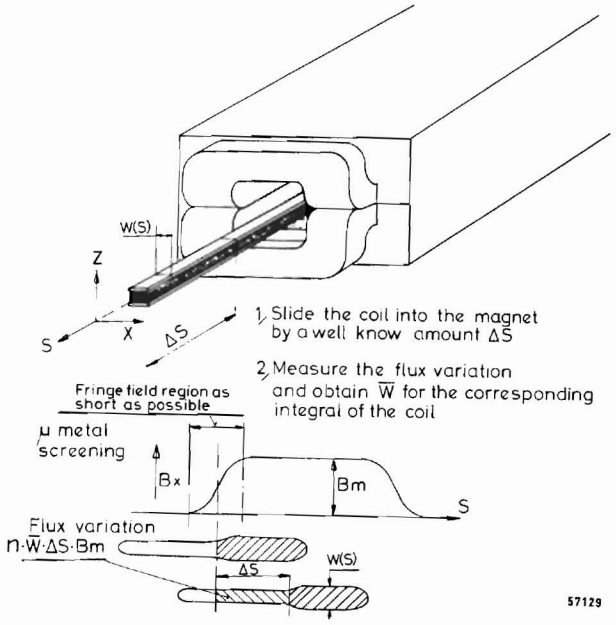

Fig. 3 Calibration in a long magnet by longitudinal displacement of the coil

c) Calibration based on a pointwise measurement of B(s), e.g. with hall probes.

We obtained absolute accuracies of 0.1%, 0.02%, and 0.01% with methods a, b, and c, respectively.

2.3 Measuring accuracy

With one recalibration every fortnight, the stability of the measuring system was:

±0.01% for absolute measurements,
±0.003% for field homogeneity measurements.

3. Measurement of the quadrupoles

3.1 Particular features of the measuring coil

As mentioned in Section 1, a harmonic coil system was used for measuring the quadrupole field parameters. This method is recommended if a) the particle beam stays within an inscribed circle touching the poles of the quadrupole, and if b) the results of the measurements have to be given in terms of multipole coefficients.

The particular features of the harmonic coil are:

i) For accurate measurements of the higher order multipoles, a compensation winding was used, as shown in Fig. 4. A compensation winding, situated at a smaller radius, has to be more sensitive than the measuring winding, so that in a pure quadrupole field the induced voltage in both of the windings is the same for any angular position. The difference voltage shows all the multipole fields except the quadrupole one.

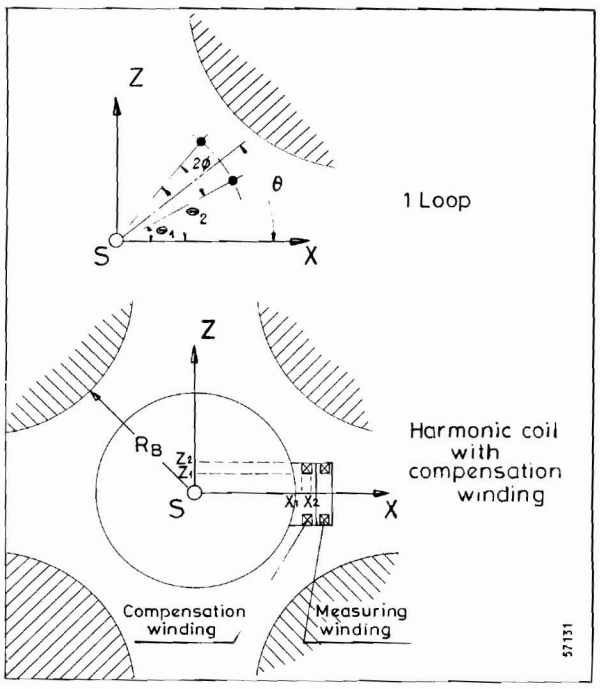

Fig. 4 Above: Flux induced in a single loop. Below: Harmonic coil with compensation winding

ii) The coil is subdivided into three parts in the longitudinal sense, so that measurements of the field inside the iron yoke and field integrals can be taken with the same measuring apparatus.

iii) The magnetic centre measurement may be performed either by the (uncompensated) harmonic coil or by a special search coil on the quadrupole axis. The second method turned out to be more accurate.

iv) Owing to the compensation method, the mechanical layout becomes very simple. There is no need for accurate angular positioning, and slip rings with the associated noise problems could be avoided.

3.2 Theory of the measurement

Using cylindrical coordinates as in Fig. 4, the general field expansion around the origin becomes:

$$\vec{B} = B_r \vec{r}_0 + B_\Theta \vec{\Theta}_0$$

$$B_r = \sum_{n=1}^{\infty} n\, a_n\, r^{n-1} \sin n\Theta + n\, b_n\, r^{n-1} \cos n\Theta$$

$$B_\Theta = \sum_{n=1}^{\infty} n\, a_n\, r^{n-1} \cos n\Theta - n\, b_n\, r^{n-1} \sin n\Theta \; . \qquad (3)$$

Only the range $r \leq R_B$ is considered, R_B being the bore radius of the quadrupole. This expansion may be applied to the bi-dimensional field in the centre of the lens or to the integrals[5]

$$\int_{-\infty}^{\infty} B_r \, ds \; ; \quad \int_{-\infty}^{\infty} B_\Theta \, ds \; .$$

The principle of harmonic coil measurements has been discussed in several papers[6]. In our case, the multipole coefficients a_n and b_n have been determined by a pointwise measurement of the function $B_r(\Theta)$.

Let us first calculate the flux Φ_ℓ induced in one loop of the coil (see Fig. 4). If ℓ is the loop length, the flux contribution of the 2n-pole field becomes:

$$\Phi_{\ell n} = \int \vec{B} \, d\vec{s} = \ell \int_{\Theta_1}^{\Theta_2} B_r \, r \, d\Theta =$$

$$= \ell \int_{\Theta_1}^{\Theta_2} \left[n\, a_n\, r^{n-1} \sin n\Theta + \right.$$

$$\left. + n\, b_n\, r^{n-1} \cos n\Theta \right] r \, d\Theta \; . \qquad (4)$$

After integration and the following substitution

$$\theta = \tfrac{1}{2}(\Theta_1 + \Theta_2) \; ; \quad \phi = \tfrac{1}{2}(\Theta_2 - \Theta_1) \qquad (5)$$

one finds

$$\Phi_{\ell n} = z\, \ell \left[a_n \sin n\theta + b_n \cos n\theta \right] r^n \sin n\phi \; . \qquad (6)$$

The loop geometry is given by the parameters r and ϕ. In order to calculate the flux of a uniformly wound coil, one has to integrate over a rectangular area with the boundaries x_1; x_2; z_1; z_2.

The integration becomes easy by introducing a complex variable $w = x + iz$:

$$r^n \sin n\phi = \mathrm{Im} \left[(x + iz)^n \right] \; . \qquad (7)$$

Let λ be the winding density (number of wires per mm^2), then the coil flux due to the 2n-pole field is:

$$\Phi_n = 2\, \ell\, \lambda \left[a_n \sin n\theta + b_n \cos n\theta \right] \times$$

$$\times \int_{z_1}^{z_2} \int_{x_1}^{x_2} \mathrm{Im}\, (x + iz)^n \, dx \, dz$$

$$= 2\, \ell\, \lambda \left[a_n \sin n\theta + b_n \cos n\theta \right] \times \frac{-1}{(n+1)(n+2)}$$

$$\times \mathrm{Re} \left[(x_2 + iz_2)^{n+2} - (x_2 + iz_1)^{n+2} - \right.$$

$$\left. - (x_1 + iz_2)^{n+2} + (x_1 + iz_1)^{n+2} \right] . \qquad (8)$$

Having measured the periodic function $\Phi(\theta) = \sum_{n=1}^{\infty} \Phi_n(\theta)$ in a certain number m of equidistant points, one can find a_n and b_n up to the order of m/2 by discrete Fourier analysis using Eq. (8). Two methods for measuring $\Phi(\theta)$ have been applied:

a) by pulsing the quadrupole field with various positions θ of the coil;
b) by stepwise rotation of the coil in a steady-state field.

3.3 Advantage of the compensation winding

Measuring errors may be introduced by the Φ-measurement (voltmeter errors and noise) and by the error in positioning or measuring of θ. Furthermore, a radial displacement Δr of the coil axis (due to play, vibration and non-cylindric bearing surfaces) will produce measuring errors. In many cases, the error due to Δr is the most important.

Let us consider the dimensionless error quantities $\Delta\Phi/\hat{\Phi}_2$; $\Delta r/r_B$ and Δ_θ [rad], where $\hat{\Phi}_2$ is the amplitude of the quadrupole flux and r_B is the quadrupole bore radius.

We assume Gaussian distribution and denote the standard deviations as σ_Φ, σ_r and σ_θ. For a simplified harmonic coil consisting of a single loop, we then calculate the measuring error (standard deviation) of the harmonic coefficients. Here also, we define dimensionless harmonic coefficients α_n, β_n representing field errors with respect to the quadrupole field at bore radius:

$$\alpha_n = \frac{n\, a_n\, r_B^{n-1}}{2\, a_2\, r_B} \; ; \quad \beta_n = \frac{n\, b_n\, r_B^{n-1}}{2\, a_2\, r_B} \; . \qquad (9)$$

After treatment with the discrete Fourier transform and Eq. (6) one obtains for the standard deviation of α_n and β_n :

$$\sigma_{\alpha n} = \sigma_{\beta n} = \left(\frac{r_B}{r_c}\right)^{n-2} \frac{n}{2} \frac{\sin 2\phi}{\sin n\phi} \times$$

$$\times \sqrt{\frac{2}{p}}\ \sqrt{\sigma_\Phi^2 + \sigma_r^2 + 2\sigma_\theta^2} \qquad (10)$$

r_c is the distance of the coil from the quadrupole centre (measuring radius) and p the number of (equidistant) measuring points.

Equation (10) illustrates several design principles:

1) Try to make $r_B/r_c \simeq 1$.

2) Avoid that $\sin n\phi \simeq 0$ for any n of interest.

3) Introducing typical numerical values ($r_B/r_c = 1.1$); $n \leq 10$; $p = 72$) we find that the measuring error on α_n and β_n is of the same order of magnitude as the individual errors σ_Φ, σ_r and σ_θ. This is of course valid for the uncompensated coil since we did the calculation for a single loop.

With the compensation winding, the measuring accuracy was improved by a factor of 100 in the present case. The reproducibility for measuring the coefficients α_n and β_n was better than ±0.003% up to n = 14. To achieve this result, it was important to keep the radial distance small between measuring winding and compensation winding. This layout reduces the influence of the error due to radial coil movements (in the present case by a factor of 8). Figure 5 gives a plot of the compensated coil voltage versus the angular position θ, showing that compensated quadrupole flux is about 0.1% of the uncompensated value so that the multipoles may be clearly distinguished.

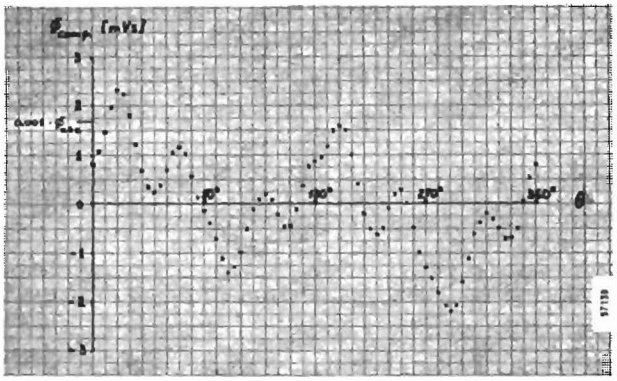

Fig. 5 Compensated coil voltage versus angular position as measured on a booster quadrupole

3.4 The measuring frame

Figure 6 shows the measuring frame with one of the booster quadrupoles. The particular feature of these quadrupoles is the four gap, single-core construction[1]). One of the most important parameter to be measured is the position of the four magnetic axes with respect to the top alignment targets. Using rotated or flipped coils for this measurement, the positions of the magnetic axis are found with respect to the coil rotation axes. This means that the bearings of the measuring coils have to be at a well known position with respect to the quadrupole targets and outside reference surfaces.

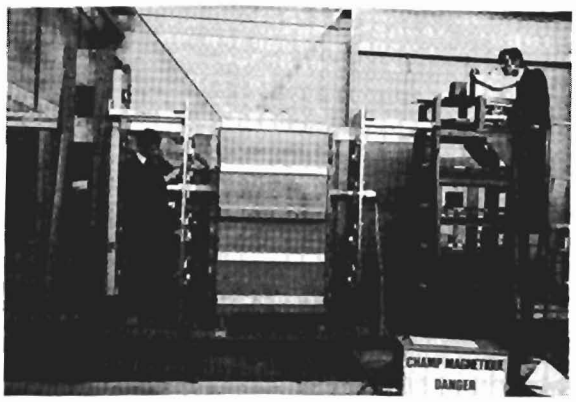

Fig. 6 Measuring frame for the booster quadrupoles

The adopted solution is a free standing frame with eight bearings which are aligned parallel and at the nominal distances. The alignment itself was done by means of an alignment telescope and two pentaprisms on the right-hand framework of

Fig. 6. By displacing the lower pentaprism, five optical axes can be established. Distances and parallelism of the axes are obtained by a system of ten optical targets built into the two outer frames. The tilt of the quadrupole, with respect to vertical target axes, is controlled by an electronic level.

The measuring tube rests on four accurately machined rollers. The tube may be put into position very quickly and the reproducibility of the tube location is of the order of a few μm.

Figure 7 shows the connection end of the measuring tube. One can distinguish the optical target, a toothed positioning gear, and the harmonic coil fixed against the outside of the tube.

Fig. 7 Measuring tube supporting the harmonic coil

Most of the measurements were performed by pulsing the quadrupole, and the coil was rotated by one increment between the pulses. This incrementing was made manually, the angular position being recorded by means of a microswitch and an electronic counter.

3.5 Performance of the system

Emphasis was put on accuracy and reliability rather than on measuring speed and sophisticated data handling, because the pure measuring time was, in any case, small compared with the time for installation and alignment of the quadrupoles.

For the magnetic centre measurement, we obtained an absolute accuracy of ±0.02 mm and a reproducibility of ±0.01 mm in an air-conditioned laboratory.

For the multipole coefficients up to n = 14, the reproducibility is better than 0.003% in terms of normalized coefficients α_n, β_n (see Eq. 9). This figure depends on the order of magnitude of the errors to be measured (see Fig. 5). Systematic errors due to coil imperfections and coil calibration errors were certainly smaller than 3% of the measured α_n, β_n. A better calibration (to be done in both dipole and quadrupole fields) is possible.

Table 1 gives a typical measuring result for a booster quadrupole. The spectrum of the α_n and β_n is in good agreement with theory. A perfectly symmetric quadrupole having a hyperbolic pole profile, which is not continued to infinity but cut off somewhere, contains the series of coefficients $\alpha_{2(2k+1)}$ (k = 1, 2, 3 ...). Symmetry distortions produce a continuous spectrum of α_n, β_n with decreasing amplitude, i.e. mainly sextupole and octupole fields.

TABLE I Multipole coefficients of a booster quadrupole

n	3	4	5	6	7	
α_n [%]	-0.006	0.021	-0.003	-0.009	-0.002	
β_n [%]	0.062	0.024	0.024	0.000	0.011	
n	8	9	10	11	12	
α_n [%]	-0.010	0.001	-0.132	0.003	-0.002	
β_n [%]	0.002	0.002	0.012	-0.003	0.002	
n	13	14	15	16	17	18
α_n [%]	0.001	-0.030	0.000	-0.001	0.004	-0.084
β_n [%]	-0.002	0.001	0.009	0.001	0.002	-0.006

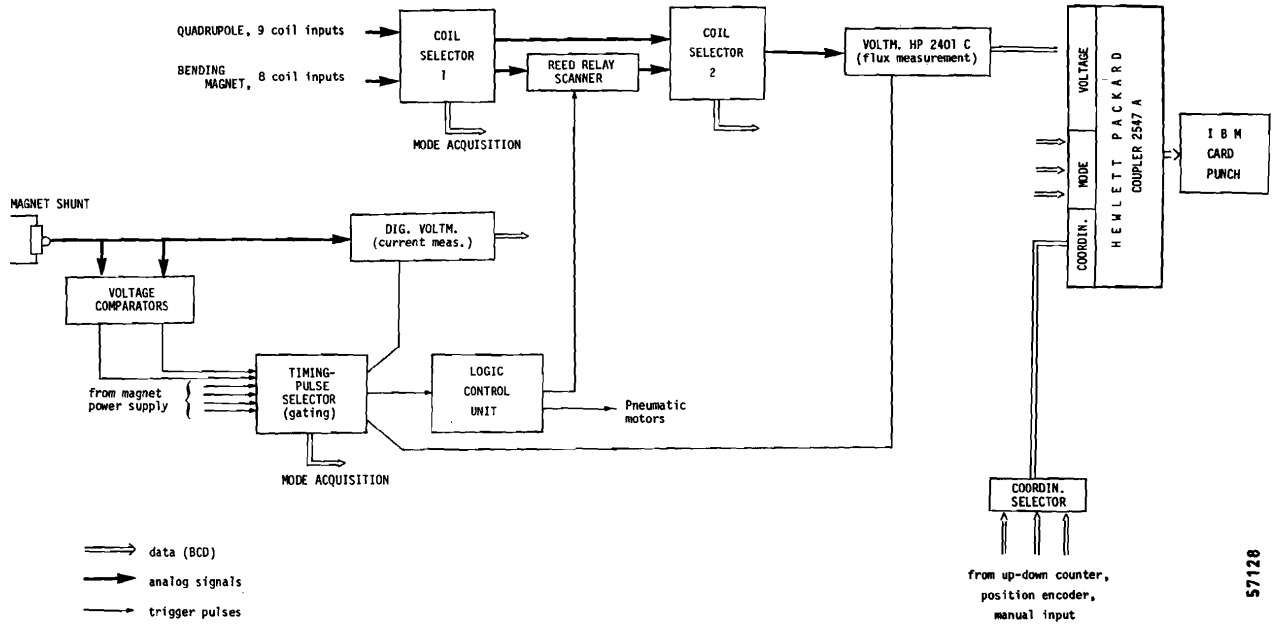

Fig. 8 Simplified block diagram of the data acquisition system

From the multipole coefficients, a field plot on any quadrupole axis (x, z, r) may be computed. This was done by our standard evaluation computer program, and the result was compared to gradient coil measurements performed on the same quadrupole unit. Taking into account multipoles up to the order n = 19, the differences are smaller than 0.015% within 90% of the quadrupole aperture.

4. Data handling

The measured data is stored on punched cards. The card punch is coupled directly to the integrating digital voltmeter, the coordinate transducers, and a measurement mode encoder giving information on:

- the measuring coil circuit (long coil/short coil, compensated/uncompensated, field coil, gradient coil, harmonic coil etc.);
- the trigger point on the current cycle.

Figure 8 shows the simplified block diagram of the data acquisition system for bending magnets and quadrupoles. As the system is fairly standard, we only mention a few particular features.

The measurement data is punched onto cards by words of 20 characters. Each word contains: voltmeter reading, measurement mode, and coordinate. In total there are 75 possible combinations of measurement modes and to avoid errors, it was essential to generate the mode information automatically from the coil selectors and the timing pulse selector.

In order to record the voltage of three coils corresponding to three z levels either three voltmeters or an analog scanner is required. For economical reasons, an analog scanner was used which is driven from a central logic control unit. This unit also controls the pneumatic flipping.

References

1) A. Asner et al., Proc. 3rd Int. Conf. on Magnet Technology, Hamburg, 1970 (DESY, Hamburg, 1970), p.418.

2) C. Bovet and K. Schindl, PSB emittance blow-up in non-linear fields, CERN Report SI/Int. DL/70-4 (1970).

3) C. Bovet et al., Proc. 8th Int. Conf. on High-Energy Accelerators, Geneva, 1971 (CERN, Geneva, 1971), p. 380.

4) H. Wind, Nuclear Instrum. Methods 84, 117 (1970).

5) W.C. Elmore and M.W. Garret, Rev. Sci. Instrum. 25, 480 (1954).

6) J.K. Cobb and D. Horelick, Proc. 3rd Int. Conf. on Magnet Technology, Hamburg, 1970 (DESY, Hamburg, 1970), p. 1439.